J Mater Sci: Mater Med (2011) 22:2813–2821
DOI 10.1007/s10856-011-4460-y

# Influence of topographical features on the fluoride corrosion of Ni–Ti orthodontic archwires

**C. Abalos · A. Paúl · A. Mendoza · E. Solano · F. J. Gil**

Received: 25 April 2011 / Accepted: 10 October 2011 / Published online: 1 November 2011


**Abstract** Different manufacturing processes of Ni–Ti archwires respond differently to corrosion due to the surface conditions involved. In this study, several topographical features and their influence upon fluoride corrosion were studied. Four topographies (smooth, dimple, scratch, and crack) according to the main surface defect were characterized (n = 40). Static corrosion tests were performed in artificial saliva with fluorated prophylactic gel (12500 ppm) for 28 days. The surface was characterized by SEM and laser confocal microscopy. Standard electrochemical corrosion (open circuit potential, corrosion potential and corrosion current density) was performed. Statistical analysis was carried out using the ANOVA test ($\alpha \leq 0.05$). An increase was observed in the surface defects and/or roughness of the cracked and scratched surfaces. These defects produced an important increase in corrosion behavior. The best surfaces for the orthodontic archwires were the smooth and dimpled surfaces, respectively. The increase in defects was independent of roughness. Manufacturing processes that produce surface cracks should be avoided in orthodontic applications.

C. Abalos
Department of Dental Materials, School of Dentistry, University of Seville, Seville, Spain

A. Paúl
Department of Mechanical and Materials Engineering, School of Engineering, University of Seville, Seville, Spain

A. Mendoza
Department of Pediatric Dentistry, School of Dentistry, University of Seville, Seville, Spain

E. Solano
Department of Orthodontics, School of Dentistry, University of Seville, Seville, Spain

F. J. Gil
Department of Materials Science and Metallurgical Engineering, Technical University of Catalonia, Barcelona, Spain

F. J. Gil (✉)
Department Ciencia de Materiales e Ingeniería Metalúrgica, Universidad Politécnica de Cataluña, Diagonal 647, 08028 Barcelona, Spain
e-mail: francesc.xavier.gil@upc.edu

## 1 Introduction

Nickel–titanium alloys (Ni–Ti) near equiatomic composition have wide clinical applications in orthodontics due to their unusual characteristics: superelasticity and shape memory effect [1, 2]. These alloys have good biocompatibility in artificial saliva, Ringer's solution and physiological saline solution [3]. Nevertheless, the corrosion resistance of Ni–Ti alloys decreases in acidic saliva [4–6] and chlorine [7] or fluoride solutions [8–12], which are frequently used in dental treatments for the prevention of caries.

Fluoride ions can deteriorate the passive film of the titanium oxide surface [9, 13–15] through hydrogen absorption [15], decreasing the corrosion resistance of the alloy and hence its biocompatibility [3, 5, 6]. Factors such as exposure time [15, 16], fluoride concentration [8, 9, 17] and a more acidic pH [15, 17] facilitate the surface corrosion of Ni–Ti alloys, since these factors are interrelated [16]. A pH dependent critical concentration has even been defined [8, 18, 19] which can degrade the passive film of surface oxides. Corrosion in HF is produced with a critical concentration of 30 ppm that destroys the $TiO_2$-based passive film on Ni–Ti archwires [20]. This concentration is reached with $\geq$500 ppm fluoride and pH = 4 [20], or with 2250 ppm fluoride in neutral solution [9]. When this happens, the effect of corrosion is a release of metal ions [5, 8, 14, 19, 21], with

morphological surface changes [8, 15, 16] and increases in the roughness [5, 8] and friction coefficients [22], among others.

Besides the aforementioned factors related to fluorine ions, the wire surface plays an important role in corrosion, although the results published to date are controversial. Previous studies [5, 21, 23, 24] point to surface defects produced during wire manufacture as preferential corrosion sites, though other studies have observed no such correlation [4, 9]. Some authors [13] consider the roughness of the archwire to be an indicator of the tendency toward corrosion, although other studies [4, 5, 8, 9] have found no such relationship when including residual stresses and the degree of homogeneity as corrosion accelerators [4, 9]. Thus, different archwire surfaces show a better or worse response to corrosive fluoride, and the archwire manufacturer therefore represents a variable in itself [4, 8]-though further research is required in this field [8, 9].

The wire surface, defects and roughness features are related to the manufacturing processes [8] that lead to different surface finishes [25]. The objective of this study, is to examine the influence of the surface (surface defects and roughness), resulting from the manufacturing process, upon the corrosion behavior of Ni–Ti archwires exposed to a high fluoride concentration. In the present study, 16 brands from different manufacturers were examined by scanning electron microscopy (SEM), and we established a topographical profile for each wire according to the main defect observed (crack, scratch, pore, dimple or smooth). The wires from different manufacturers were grouped according to the topographical feature corresponding to the different manufacturing processes involved, and two of them corresponding to each topography were selected. We analyzed the influence of each topographical feature on fluoride corrosion behavior by means of a surface study (SEM) and the assessment of roughness (laser confocal microscopy).

## 2 Materials and methods

### 2.1 Preliminary study

The surfaces of 16 Ni–Ti archwires (0.016 × 0.022 inch) from nine commercial brands in the as-received condition were studied [26]. The surface morphology and composition were evaluated by SEM (Philips XL-30 Philips, Eindhoven, Netherlands) and energy dispersive spectrometry (EDS) (Edax International, Mahwah, USA). Roughness was measured using a laser scanning confocal microscope system (LSCM) (Leica TCS-SP2, Wetzlar, Germany). Three samples from each batch of archwires were analyzed, each sample coming from a different archwire within the batch. The archwires were classified according to their topographical features using 18 variables. The Pearson correlation test was performed to evaluate the existence of linear correlations between the variables. As a result, Ni–Ti archwires according to five surfaces types were classified depending on the main surface defects involved: porous, dimple, scratch, crack, and

**Table 1** Archwires used in the preliminary and experimental studies

| ARCHWIRE | COMPANY | BATCH | COMPOSITION[a] | TOPOGRAPHY |
|---|---|---|---|---|
| **Reflex superelastic**[b] | **TPO** | **1567027** | **52.9/47.1** | **Smooth** |
| **Nitinol classic**[b] | **3 M-Unitek** | **V5304** | **53.0/47.0** | **Smooth** |
| **Orthonol**[b] | **RMO** | **A07005** | **52.9/47.1** | **Dimple** |
| **Align XF**[b] | **Ormco** | **030880842** | **53.4/46.6** | **Dimple** |
| NitiCu 35 | Ormco | 07E278E | 47.2/46.5/6.3[c] | Dimple |
| **Memoria**[b] | **Leone** | **07132601** | **54.0/46.0** | **Crack** |
| **Titanol superelastic**[b] | **Forestadent** | **28636946** | **53.9/46.1** | **Crack** |
| **Tensic**[b] | **Dentaurum** | **54301** | **56.5/43.4** | **Scratch** |
| **Nitinol HA**[b] | **3M-Unitek** | **AP1FY** | **53.0/47.0** | **Scratch** |
| Ramatitan Lite | Dentaurum | 60648 | 54.5/45.5 | Scratch |
| G4 | G&H | 142669 | 53.3/46.7 | Scratch |
| M5 | G&H | 126755 | 53.3/46.6 | Scratch |
| Thermomemoria | Leone | 08022001 | 53.9/46.1 | Scratch |
| Thermaloy | RMO | A07304 | 53.4/46.6 | Scratch |
| Reflex heat-activated | TPO | 1297060 | 53.2/46.7 | Scratch |
| Neo sentalloy | GAC | H326 | 53.1/46.8 | Porous |

[a] %Ni/%Ti (wt%)

[b] Archwires used in the experimental study (in bold)

[c] %Ni/%Ti/%Cu (wt%)

smooth (Table 1). These defects are not exclusive of each topographical profile. The *smooth topography* (Fig. 1a) has few defects, with an absence of cracks, and exhibits medium–low roughness. The *dimple topography* (Fig. 1c) is characterized by the presence of dimples and some pores, together with the absence of scratches. It is associated with important roughness. The *crack topography* (Fig. 1e) always presents pores and is the only topographical profile showing inclusions (arrow in micrograph inset in Fig. 1e), fundamentally Al. Lastly, the *scratch topography* (Fig. 1g)

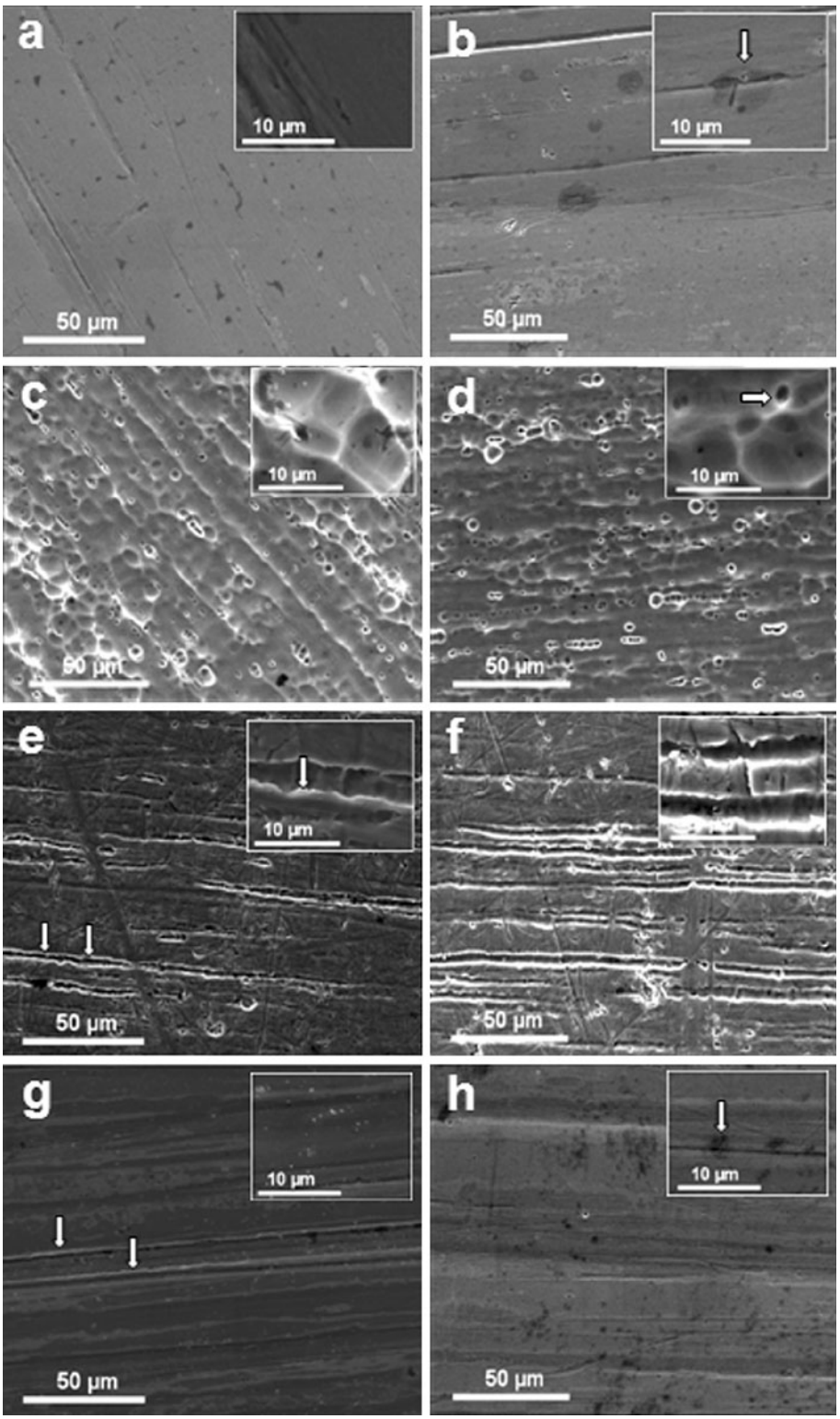


**Fig. 1** Representative SEM images of Ni–Ti wires (×400 and inset ×1600 magnification). As-received topography in *left column* **a** smooth, **c** dimple, **e** crack (arrow in ×1600 image indicates inclusion), and **g** scratch. Fluor-treated topography in *right column* **b** smooth (*arrow* pitting corrosion), **d** dimple (*arrow* pore), **f** crack and **h** scratch (*arrow* circular spot)

is the most frequent topographical type. Besides scratches, all have some pores and cracks, and roughness is medium–low. The porous topography was discarded for the study, since it was found in only one archwire.

The different surface defects were defined as follows: a *crack* is a long, deep fissure with irregular edges and variable width (arrow in Fig. 1e); a *dimple* is a small hole, an elliptical or rounded depression on the surface similar to the dimples in a golf ball (micrograph inset in Fig. 1c); a *pore* is a deep, usually rounded defect (arrow in micrograph inset Fig. 1d); a *micropore* is a pore with diameter smaller than one micrometer; and a *scratch* is a long fissure with smooth edges and constant width, in which the bottom is clearly visible (arrows in Fig. 1g).

### 2.2 Material and static corrosion test

Eight Ni–Ti wires with near equiatomic compositions made by different manufacturers were used in this study. Each topographical feature (crack, dimple, scratch, and smooth) was represented by two different commercial brands (Table 1). For the tests, we used five samples of different archwires from the same batch (n = 40). The samples were 20 mm segments extracted from the straight part of the arch. Prior to static corrosion testing, each specimen was cleaned and degreased for 5 min in acetone.

In order to simulate the intraoral conditions of the wires, the samples were placed in a polypropylene (PP) tube (15 ml) with 2 ml artificial saliva for 28 days at 37°C. Modified Fusayama artificial saliva was used, with the following composition: NaCl (0.4 g/l), KCl (0.4 g/l), $CaCl_2{\cdot}2H_2O$ (0.906 g/l), $NaH_2PO_4{\cdot}H_2O$ (0.690 g/l), $Na_2S{\cdot}9H_2O$ (0.005 g/l), KSCN (0.3 g/l) and urea (1 g/l). [5, 6, 9, 10]. The pH was measured by means of a pH-meter (micropH 2001, Crison Instrument S.A., Barcelona, Spain) yielding a value of 5.3. The recommendations of the manufacturer for brushing with high concentration fluor gel (Elmex gel, GABA GmbH, Lörrach, Germany) was 1–2 min per week. Accordingly, the samples were placed for 2 min a week (8 min in total) in a 15 ml PP tube with 2 ml artificial saliva with fluoride solution. The fluoride solution was prepared by ultrasonic agitation in the PP tube of 5 ml artificial saliva and 5 g fluorated prophylactic gel (12500 ppm); the mixture was centrifuged for 10 min at 2,000 rpm. The upper clear liquid without the deposits in the PP tube was used for the static corrosion test [8]. The pH of this solution was four, and it was used at 37°C. Immediately after the static corrosion test, the samples were rinsed for 5 min in distilled water and for 5 min in methanol in a stirrer maintained at the testing temperature of 37°C.

### 2.3 Surface characterization

The surface topography of the Ni–Ti archwires was examined before and after the static corrosion tests. SEM micrographs were taken of representative degraded areas of the surface. We used the images to measure the surface occupied by each defect (dimples, cracks and pores) in three different areas of 10,000 $\mu m^2$. The three measurements were then averaged. Accordingly, five samples per brand of wire (n = 40) and three areas per specimen were measured. In the case of the scratches, in each sample we measured the millimeters they occupied in ten different lines measuring 100 μm. These ten measurements were then averaged.

Surface roughness of the Ni–Ti archwires was analyzed before and after the static corrosion tests by means of LSCM. The microscope was previously calibrated using a Mitutoyo precision Reference Specimen (Code no. 178-601) with Ra = 3.1 μm, the error coefficient being under 0.3%. The images were processed using Leica Confocal software (Leica *Microsystems* GMBH, Wetzlar, Germany). Micrographs corresponding to a fragment of wire measuring 750 μm (750 × 450 μm, approximately) were taken. We randomly selected five areas of 10,000 $\mu m^2$ from each topographic image and measured the roughness. *Ra*, *Rms*, *Rp and Rv* values obtained in each area were averaged. *Ra* and *Rms* represent the arithmetical mean of the absolute values and the root-mean-square value of the scanned surface profile, respectively. *Rp* and *Rv* represent the upper and lower values of the scanned profile. Thus, for roughness studies, we analyzed five areas from five samples of each archwire (n = 40). Roughness calculation was based on the DIN EN ISO 4287 norm.

### 2.4 Corrosion tests

Archwires were sectioned in order to yield corrosion testing samples. A 25 mm length of each archwire was cut with sterile orthodontic pliers and isolated with wax (Paraffin wax Sigma Aldrich) at the interphase between the testing solution and air. The corrosion tests were performed following the ISO-standard 10993-15:2000 "Biological evaluation of medical devices. Part 15: Identification and quantification of degradation products from metals and alloys".

The tests were carried out with a Voltalab PGZ 301 potentiostat (Radiometer, Copenhagen, Denmark) controlled by Voltamaster 4 software (Radiometer Analytical, Villeurbanne Cedex, France). The testing solution was artificial saliva and artificial saliva with fluoride solution kept at a controlled constant temperature of 37°C. The reference electrode was an Ag/AgCl/KCl electrode ($E^\circ$ = 0.222 V). The auxiliary electrode used was a

platinum electrode with a surface of 240 $mm^2$ (Radiometer Analytical, Villeurbanne, France).

In the corrosion tests we defined the following: (a) *Open circuit potential* ($E_{OCP}$), the potential of an electrode measured with respect to a reference electrode or another electrode when no current flows to or from the material; (b) *corrosion potential* ($E_{CORR}$), the potential calculated at the intersection where the total oxidation rate is equal to the total reduction rate; and (c) *corrosion current density* ($i_{CORR}$), the current divided by the surface of the electrode. It is the size of the anodic component of the current which flows at the corrosion potential $E_{CORR}$.

The open circuit potential ($E_{ocp}$) was monitored for 3 h in order to allow leveling-off of the value before the polarization resistance test. The cyclic voltammetry assay was performed by scanning the potential of the alloy of the sample at 0.25 mV/s with the minimum current set at −1 A and the maximum at +1 A, with a minimum range set at 100 μA between −300 and +2000 mV around the OCP value. The open circuit potentials ($E_{ocp}$), corrosion potentials ($E_{corr}$) and corrosion currents ($i_{corr}$) were recorded for the different samples tested.

### 2.5 Statistical analysis

Mean values and standard deviations of each of the eight brands and the four surface topography features were computed from the data obtained during surface characterization. This was done for the as-received archwires as well as after the corrosion test. Since the archwires used had different initial values, in order to ensure valid comparison of the statistical results, we deemed it appropriate to use the difference between the post-static corrosion test and the as-received values obtained for each wire tested. Thus, the final values refer to the increases or decreases in the area occupied by the surface defects (Δ Def), surface roughness (Δ Ra, Δ Rms) or electrochemical corrosion testing (Δ Ecorr, Δ icorr, Δ $E_{OCP}$). Positive values imply surface degradation, while zero or negative values indicate the absence of corrosion. Statistical analysis was carried out using analysis of variance (ANOVA) for the comparison of mean values, with correction using Bonferroni's post hoc test. Statistical significance was set at $\alpha \leq 0.05$. The data were analyzed using the SPSS version 14.0 statistical package (SPSS Inc., Chicago, IL, USA).

## 3 Results

Table 2 shows the results corresponding to the surface occupied by each type of defect in the as-received archwires. Also shown are the mean and standard deviation of the increase in defects (Δ Def) for each topographical feature category (smooth, dimple, crack, scratch), following the static corrosion test. Δ Def was seen to be greater in the topography with cracks, showing statistically significant differences with respect to the remaining topographical features. Figure 1 shows representative SEM images of the changes in the surface of the four topographies after the corrosion tests. In the crack topography, a 6.3% increase (Table 2) in the surface occupied by the defects was observed, mainly due to the increased surface of the cracks (Fig. 1f). In the dimple topography there was no pitting or discoloration, and a smoothing of the surface was observed (Fig. 1d). Consequently, the surface reduces the number of defects present (Table 2). In the scratch topography there were also some circular spots (arrow in micrograph inset in Fig. 1h), while the smooth topography showed pitting

**Table 2** Surface area of the defects and variation (Δ Def, obtained by subtracting average total defects) before and after static corrosion testing in saliva + fluoride

| Ni–Ti Archwires | MANUFACTURING DEFECTS | | | | | | TOPOGRAPHY FEATURES | Δ Def SALIVA + F | |
|---|---|---|---|---|---|---|---|---|---|
| | Cracks[a] | Pores[a] | μPores[a] | Scratches[b] | Dimples[a] | Total | | Mean | SD |
| Reflex SE | 0 | 0 | 0.008 | 2.9 | 0 | 2.908 | Smooth | 0.398 | 0.246 |
| Nitinol classic | 0 | 1.74 | 0.019 | 0 | 0.25 | 2.009 | | | |
| Orthonol | 0 | 2.28 | 0.015 | 0 | 62.15 | 64.445 | Dimple | −1.44 | 0.48 |
| Align XF | 0.737 | 2.58 | 0.033 | 0 | 13.02 | 16.37 | | | |
| Memoria | 5.775 | 0.051 | 0.017 | 1.28 | 1.76 | 8.883 | Crack | **6.313**[‡] | 0.680 |
| Titanol SE | 2.645 | 0.356 | 0.013 | 0 | 0 | 3.014 | | | |
| Tensic | 0.07 | 0 | 0 | 6.8 | 0.003 | 6.873 | Scratch | 0.517 | 0.316 |
| Nitinol HA | 0.579 | 0.588 | 0.077 | 13 | 1.38 | 15.624 | | | |

Crack topography shows statistically significant Δ Def with respect to the rest of the topographies (in bold)

[a] % area of defects in the sample

[b] μm per 100 μm in linear scratches

[‡] Mean significant difference ($P < 0.05$) by ANOVA Bonferroni post hoc test

**Table 3** Surface roughness data and variation (ΔRa and ΔRms, obtained by subtracting average Ra and Rms) before and after static corrosion testing in saliva + fluoride

| Ni–Ti Archwires | SURFACE ROUGHNESS AS-RECEIVED | | | | | | | VARIATION ROUGHNESS AFTER CORROSION TEST | |
|---|---|---|---|---|---|---|---|---|---|
| | Ra | Rms | Rv | Rp | TOPOGRAPHY | Ra | Rms | ΔRa | ΔRms |
| Reflex SE | 0.22 (0.06)* | 0.31 (0.08) | 2.31 (0.42) | 1.20 (0.36) | Smooth | 0.32 (0.13) | 0.45 (0.18) | 0.03 (0.01) | 0.03 (0.01) |
| Nitinol classic | 0.46 (0.04) | 0.61 (0.06) | 3.46 (0.31) | 2.76 (0.13) | | | | | |
| Orthonol | 1.32 (0.14) | 1.71 (0.18) | 8.45 (0.1) | 4.53 (0.75) | Dimple | 1.01 (0.35) | 1.35 (0.47) | −0.06 (0.02) | −0.08 (0.02) |
| Align XF | 0.70 (0.08) | 0.95 (0.16) | 7.60 (0.05) | 4.09 (0.45) | | | | | |
| Memoria | 0.44 (0.11) | 0.60 (0.15) | 4.30 (0.31) | 2.23 (0.59) | Crack | 0.35 (0.13) | 0.48 (0.17) | **0.13**† (0.04) | **0.19**† (0.06) |
| Titanol SE | 0.25 (0.05) | 0.37 (0.07) | 3.33 (0.77) | 1.18 (0.34) | | | | | |
| Tensic | 0.34 (0.06) | 0.47 (0.07) | 3.87 (0.99) | 1.87 (0.70) | Scratch | 0.30 (0.09) | 0.40 (0.13) | **0.10**† (0.03) | **0.14**† (0.04) |
| Nitinol HA | 0.26 (0.03) | 0.36 (0.04) | 3.14 (0.88) | 1.81 (0.63) | | | | | |

Scratch and crack topographies show statistically significant variation in roughness with respect to the rest of topographies (in bold)

* Standard deviations are given in parentheses

† Mean significant difference ($P < 0.05$) by ANOVA Bonferroni post hoc test

**Table 4** Mean values and standard deviations obtained from potentiostatic polarization plot of dental materials studied in artificial saliva solution

| NiTi archwires | | Artificial saliva | | | Artificial saliva + Fluoride | | |
|---|---|---|---|---|---|---|---|
| | | $i_{corr}$ (μA/cm$^2$) | $E_{CORR}$ (mV) | Eocp (mV) | $i_{cr}$ (μA/cm$^2$) | $E_{CORR}$ (mV) | Eocp (mV) |
| Reflex SE | Smooth | −3.85 (0.11) | −520 (15.4) | +555 (16.4) | −2.67 (0.06) | −604 (28.1) | +540 (19.3) |
| Nitinol classic | Smooth | −3.00 (0.09) | −515 (16.3) | +568 (13.1) | −2.74 (0.08) | −620 (26.5) | +504 (21.2) |
| Orthonol | Dimple | −1.67 (0.05) | −565 (12.9) | +450 (11.7) | −1.08 (0.03) | −712 (32.1) | +489 (15.5) |
| Align XF | Dimple | −0.88 (0.03) | −579 (14.7) | +520 (15.1) | −0.78 (0.03) | −734 (25.7) | +498 (17.9) |
| Memoria | Crack | −1.36 (0.06) | −624 (16.7) | +401 (12.8) | −0.98 (0.03) | −876 (25.4) | +399 (16.7) |
| Titanol SE | Crack | −0.67 (0.05) | −657 (13.2) | +321 (13.16) | −0.01 (0.001) | −890 (34.7) | +389 (15.9) |
| Tensic | Scratch | −0.22 (0.01) | −708 (17.7) | +320 (7.68) | +0.23 (0.01) | −904 (44.4) | +267 (8.01) |
| Nitinol HA | Scratch | −0.59 (0.15) | −606 (12.8) | +290 (8.99) | +0.44 (0.01) | −987 (39.2) | +301 (13.0) |

corrosion and dark circular spots (arrow in micrograph inset in Fig. 1b).

The surface roughness data (LSCM) of the archwires in the as-received condition are expressed in Table 3. Also shown are the mean and standard deviation of the increase or decrease in roughness (ΔRa and ΔRms) for each topographic category (smooth, dimple, crack, scratch), following static corrosion testing. The increase in roughness was greater for the crack and scratch topographies, with statistically significant differences versus the smooth and dimple topographies. There was a 33% increase in surface roughness in the crack topography, with Ra changes from 0.3 to 0.4 μm after static corrosion testing. In the case of the scratch topography, Ra increased from 0.35 to 0.48 μm. Figure 2 shows representative LSCM images of the four topographical features studied.

The results obtained for Ecorr, icorr and $E_{OCP}$ during corrosion testing are presented in Table 4. The archwires tested in artificial saliva showed clearly higher resistance to corrosion than those tested in artificial saliva with fluoride solution. For the smooth archwires, the difference in $E_{corr}$ due to immersion in fluoride solution was about 100 mV. However, for the surface with dimples the differences was about 150 mV, versus around 200 mV for the crack and scratch surfaces.

The archwires with scratches and cracks showed the highest tendency towards corrosion, with average values of −650 mV in artificial saliva and −850 mV in fluoride solution. The archwires with smooth surfaces were found to be more resistant to corrosion, with Ecorr −515 and −610 mV in artificial saliva and fluoride solution, respectively.

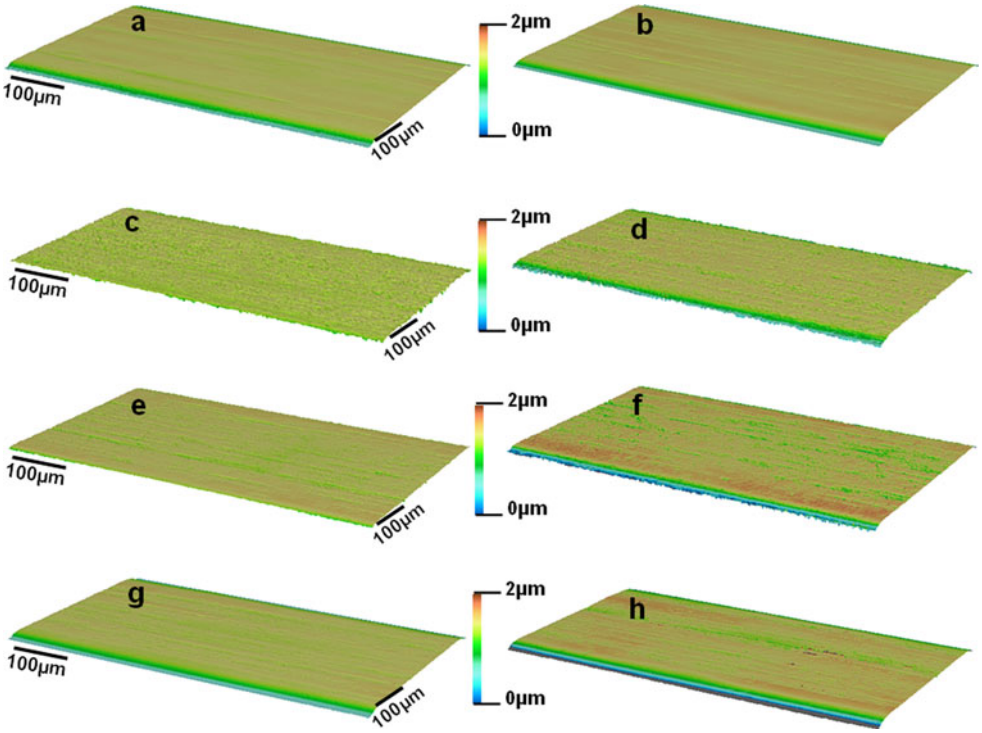


**Fig. 2** Representative LSCM images of NiTi wires. As-received topography in *left column* **a** smooth, **c** dimple, **e** crack, and **g** scratch. Fluor-treated topography in *right column* **b** smooth, **d** dimple, **f** crack and **h** scratch

Current density showed minimum values for the smooth topography (−3.85 to −3.0 μA/cm$^2$) and maximum values for the scratched topography (−0.59 to −0.22 μA/cm$^2$) in artificial saliva. The presence of fluoride solution produced an important decrease in both types of surface (between 0.5 and 1μA/cm$^2$). The open current potential values showed great variability among the measurements made, though the smooth and dimple topography values were higher than for the crack and scratch surfaces.

## 4 Discussion

There is general agreement in the literature that the archwire manufacturer exerts a statistically significant influence on corrosion resistance [4, 5, 9, 21]. However, there is some controversy regarding surface defects [4, 5, 9, 21, 23, 24] and/or roughness [4, 5, 8, 9] as the causes of corrosion. These studies compared archwires with different surface finishes, but the authors failed to specify the main topographical features, and in some cases the Ni–Ti alloys presented important differences in chemical composition, and the roughness was not determined. In the present study the Ni–Ti archwires showed very similar chemical compositions, though with different types of defects. The results obtained reveal a clear influence of the topographical features upon corrosion, as determined especially in fluoride solution.

In our study, a cracked and scratched topography presented greater corrosion behavior, possibly due to higher residual stress and/or non-uniform passive film on the surface defects [5]. According to some authors [27], cracks on the surface of the archwire are due to mechanical polishing with large particles, and are the cause of the chemical heterogeneity observed after heat treatment-inducing non-uniform deformation of surface sub-layers associated with grinding. A scratched topography receives its final form after drawing or rolling, these being processes that can leave scratches or irregularities on the surface [28]. Mechanical polishing also causes scratches. In this sense, it produces more scratching than electropolishing, with a heterogeneous surface enriched in Ni [29]. According to these authors [27], defects resulting from plastic deformation, and the non-uniform character of deformation associated with the abrasion procedure, reduce surface stability and corrosion resistance.

In our study, other surfaces presented higher corrosion resistance, such as the smooth and dimple topographies. In the case of the smooth topography, the uniform surfaces are obtained by drawing [30], followed by electropolishing. These techniques give rise to enhanced corrosion resistance [31]. In the case of the dimple topography, during archwire manufacture the surface is subjected to chemical etching in acid solutions to eliminate surface scratches, remove highly deformed defect material, oxidize the surface, and leach nickel produced after heat treatment [27]. Chemical

etching induces the formation of dimples and pores with a chemically stable surface [27]. Chemical etching and water boiling moreover successfully prevent surface enrichment in Ni [29].

After immersion in fluoride solution, we observed an increase in the surface defects in the archwires with cracks as topographical feature, but not in those with smooth, scratch or dimple surface marks. The increased number of defects was due to an increase in the number and size of the cracks. In previous studies [5, 21, 23, 24], preexisting defects were identified as corrosion sites. In the same way, studies on archwires with polished surfaces have found less corrosion [24, 32]. The preexisting surface marks provide answers regarding the variability of the corrosion resistance of different Ni–Ti archwires with near equiatomic compositions.

In our study, we used an amine fluoride gel solution with a concentration of 1.25% (12,500 ppm) and pH = 4 as the immersion medium. Thus, the solution used in our study is justified by its high concentration and acid pH, ensuring its corrosive effect. Different kinds of fluoride solutions (stannous fluoride, sodium fluoride, etc.) have different degrees of corrosiveness [18, 19]; thus, the influence of fluoride solution upon the topographical features of orthodontic archwires could be the subject of future research.

The most frequent consequences of fluoride application are pitting corrosion and changes in color. Several authors [7, 14–16] described pitting corrosion as a general attack. In our study, we only observed this with the smooth and dimple topographies (Fig. 1b, d), and in some samples with a scratch topography. Regarding the changes in color, we found dark, rounded stains on the smooth and scratch surfaces (Fig. 1b, h), in agreement with other authors [17]. We also found dark spots that disappeared after the static corrosion tests in the as-received archwires. Other authors [15–17, 30, 33, 34] have also described these discolorations. Nevertheless, we did not find the white spots or the bright white spots, which appear to be inclusions in the wire, described in other studies [11, 14–16].

Regarding the increase in roughness after immersion in fluoride, we found correlations between the cracked and scratched topographies. A number of authors [4, 5, 9] have studied the influence of initial as-received archwire roughness in relation to corrosion resistance. The results of these studies [4, 5, 9] indicate that important initial roughness is not related to lesser corrosion resistance. Our findings are in agreement with these results, since the dimple topography, with high initial roughness, did not significantly affect the number of defects, roughness or the electrochemical corrosion test results. However, the increase in roughness after static corrosion testing is related to corrosion resistance [5, 7, 8].

In the present study, an increase in roughness was not related in all cases to an increase in the number of defects, as in the scratched topography. The explanation is that the surface occupied by the defects in the scratched archwires is about 10% of the total surface, with no significant increase after static corrosion testing. Thus, roughness depends not only on the number of defects but also on the remaining surface free of defects, taking into account that immersion in fluoride solution causes a generalized increase in roughness, dependent upon the concentration and pH [7, 8].

It should be noted that the potentials in an open circuit of the all archwires adopted positive values, and consequently the studied Ni–Ti archwires remained within their immunity range. A higher current density at a given potential causes the material to be more susceptible to corrosion. The smooth and dimple topographies showed the most passive (−2.67, −2.74 and −1.08, −0.78 $\mu A/cm^2$) and the scratch topography the most active (+0.23, +0.44 $\mu A/cm^2$) critical current density values in artificial saliva with fluoride solution.

The oxide that forms on titanium provides corrosion resistance under static conditions, and it has often been reported that Ni–Ti is not susceptible to pitting and/or crevice corrosion phenomena. However, it should be pointed out that the oxide film is not sufficiently stable to prevent etching with fluoride solutions. Thus, under these conditions, the titanium oxide can be removed, resulting in the release of metallic debris and ions. These properties could represent limitations in relation to certain dental applications.

Statistically significant differences ($\alpha \leq 0.05$) between artificial saliva and fluoride containing artificial saliva were found in all the corrosion parameters shown in Table 4. The corrosion resistance of Ni–Ti alloys affects their biocompatibility and bio functionality, which are two absolute requirements for an ideal biomaterial.

For these reasons, the orthodontic archwire manufacturing process is very important for excellent long-term behavior. The manufacturers must avoid defects, especially scratched and cracked topographies.

## 5 Conclusions

Orthodontic archwires present different surface defects, depending on the manufacturing process involved. Based on the predominant defect, different topographical features can be found. A correlation between surface topography and fluoride corrosion was recorded, in the following order: (1) The cracked topography showed the most corrosion-prone behavior: high electrochemical corrosion potential, increased roughness and increased crack size; (2) The scratched topography in turn showed a high

electrochemical corrosion potential, and increased roughness; and (3) The dimpled and smooth topographies were the most corrosion resistant in that medium. In the face of a lack of manufacturing standards, those manufacturing processes that cause cracks and scratches should be avoided.

**Acknowledgments** The authors thank Dr. Juan Luis Ribas (LSCM expert) and the Center for Technology and Innovation Research, University of Seville (CITIUS), for their contribution to this study. The Spanish Ministry of Science and Innovation provided financial support of a part of this study through project MAT2009-13547.

## References

1. Kusy RP. A review of contemporary archwires: their properties and characteristics. Angle Orthod. 1997;67(3):197–207.
2. Torrisi L. The Ni–Ti superelastic alloy application to the dentistry field. Biomed Mater Eng. 1999;1:39–47.
3. Wever DJ, Veldhuizen AG, de Vries J, Busscher HJ, Uges DR, van Horn JR. Electrochemical and surface characterization of a nickel–titanium alloy. Biomaterials. 1998;19(7–9):761–9.
4. Huang HH. Variation in corrosion resistance of nickel–titanium wires from different manufacturers. Angle Orthod. 2005;75(4):661–5.
5. Huang HH, Chiu YH, Lee TH, Wu SC, Yang HW, Su KH, et al. Ion release from Ni–Ti orthodontic wires in artificial saliva with various acidities. Biomaterials. 2003;20:3585–92.
6. Wang J, Li N, Rao G, Han EH, Ke W. Stress corrosion cracking of Ni–Ti in artificial saliva. Dent Mater. 2007;23(2):133–7.
7. Li X, Wang J, Han EH, Ke W. Influence of fluoride and chloride on corrosion behavior of Ni–Ti orthodontic wires. Acta Biomater. 2007;3(5):807–15.
8. Huang HH. Variation in surface topography of different Ni–Ti orthodontic archwires in various commercial fluoride-containing environments. Dent Mater. 2007;23(1):24–33.
9. Lee TH, Huang TK, Lin SY, Chen LK, Chou MY, Huang HH. Corrosion resistance of different nickel–titanium archwires in acidic fluoride-containing artificial saliva. Angle Orthod. 2010;80(3):547–53.
10. Kwon YH, Cheon YD, Seol HJ, Lee JH, Kim HI. Changes on Ni–Ti orthodontic wired due to acidic fluoride solution. Dent Mater J. 2004;23(4):557–65.
11. Ramalingam A, Kailasam V, Padmanabhan S, Chitharanjan A. The effect of topical fluoride agents on the physical and mechanical properties of Ni–Ti and copper Ni–Ti archwires. An in vivo study. Aust Orthod J. 2008;24(1):26–31.
12. Kwon YH, Jang CM, Jang JH, Park JH, Kim TH, Kim HI. Effect of fluoride released from fluoride-containing dental restoratives on Ni–Ti orthodontic wires. Dent Mater J. 2008;27(1):133–8.
13. Widu F, Drescher D, Junker R, Bourauel C. Corrosion and biocompatibility of orthodontic wires. J Mater Sci Mater Med. 1999;10(5):275–81.
14. Schiff N, Grosgogeat B, Lissac M, Dalard F. Influence of fluoride content and pH on the corrosion resistance of titanium and its alloys. Biomaterials. 2002;23(9):1995–2002.
15. Yokoyama K, Kaneko K, Moriyama K, Asaoka K, Sakai J, Nagumo M. Hydrogen embrittlement of Ni–Ti superelastic alloy in fluoride solution. J Biomed Mater Res A. 2003;65(2):182–7.
16. Walker MP, White RJ, Kula KS. Effect of fluoride prophylactic agents on the mechanical properties of nickel–titanium-based orthodontic wires. Am J Orthod Dentofac Orthop. 2005;127(6):662–9.
17. Watanabe I, Watanabe E. Surface changes induced by fluoride prophylactic agents on titanium-based orthodontic wires. Am J Orthod Dentofac Orthop. 2003;123(6):653–6.
18. Schiff N, Boinet M, Morgon L, Lissac M, Dalard F, Grosgogeat B. Galvanic corrosion between orthodontic wires and brackets in fluoride mouthwashes. Eur J Orthod. 2006;28(3):298–304.
19. Schiff N, Grosgogeat B, Lissac M, Dalard F. Influence of fluoridated mouthwashes on corrosion resistance of orthodontics wires. Biomaterials. 2004;25(19):4535–42.
20. Nakagawa M, Matsuya S, Shiraishi T, Ohta M. Effect of fluoride concentration and pH on corrosion behavior of titanium for dental use. J Dent Res. 1999;78(9):1568–72.
21. Es-Souni M, Es-Souni M, Fischer-Brandies H. On the properties of two binary Ni–Ti shape memory alloys. Effects of surface finish on the corrosion behaviour and in vitro biocompatibility. Biomaterials. 2002;23(14):2887–94.
22. Wichelhaus A, Geserick M, Hibst R, Sander FG. The effect of surface treatment and clinical use on friction in Ni–Ti orthodontic wires. Dent Mate. 2005;21(10):938–45.
23. Oshida Y, Sachdeva RC, Miyazaki S. Microanalytical characterization and surface modification of TiNi orthodontic archwires. Biomed Mater Eng. 1992;2(2):51–69.
24. Trepanier C, Tabrizian M, Yahia LH, Bilodeau L, Piron DL. Effect of modification of oxide layer on Ni–Ti stent corrosion resistance. J Biomed Mater Res. 1998;43(4):433–40.
25. Es-Souni M, Fischer-Brandies H, Kock N, Bock O, Rätzke K. Chemische Zusammensetzung, Umwandlungsverhalten und mechanische Biegeeigenschaften ausgewählter kieferorthopädischer Ni–Ti-Drahtbögen. IOK. 2001;33:87–106.
26. Paúl A, Ábalos C, Mendoza A, Solano E, Gil FJ. Relationship between the surface defects and the manufacturing process of orthodontic Ni–Ti archwires. Mater Lett. 2011;65(1):3358–3361.
27. Shabalovskaya SA, Anderegg J, Laab F, Thiel PA, Rondelli G. Surface conditions of nitinol wires, tubing, and as-cast alloys. The effect of chemical etching, aging in boiling water, and heat treatment. J Biomed Mater Res B Appl Biomater. 2003;65(1):193–203.
28. Prososki RR, Bagby MD, Erickson LC. Static frictional force and surface roughness of nickel–titanium arch wires. Am J Orthod Dentofac Orthop. 1991;100(4):341–8.
29. Shabalovskaya S, Anderegg J, Van Humbeeck J. Critical overview of Nitinol surfaces and their modifications for medical applications. Acta Biomater. 2008;4(3):447–67.
30. Grimsdottir MR, Hensten-Pettersen A. Surface analysis of nickel–titanium archwire used in vivo. Dent Mater. 1997;13(3):163–7.
31. Wu W, Liu X, Han H, Yang D, Lu S. Electropolishing of NiTi for improving biocompatibility. J Mater Sci Tech. 2008;24:926–30.
32. Hunt NP, Cunningham SJ, Golden CG, Sheriff M. An investigation into the effects of polishing on surface hardness and corrosion of orthodontic archwires. Angle Orthod. 1999;69(5):433–40.
33. Huang HH. Surface characterizations and corrosion resistance of nickel–titanium orthodontic archwires in artificial saliva of various degrees of acidity. J Biomed Mater Res A. 2005;74(4):629–39.
34. Eliades T, Eliades G, Athanasiou AE, Bradley TG. Surface characterization of retrieved Ni–Ti orthodontic archwires. Eur J Orthod. 2000;22(3):317–26.